

1 **Cooperative Effects of RIG-I-like Receptor Signaling and IRF1 on DNA Damage-Induced**  
2 **Cell Death**

3

4 David Y. Zander<sup>1,2</sup>, Sandy S. Burkart<sup>1,3</sup>, Sandra Wüst<sup>1</sup>, Vladimir G. Magalhães<sup>1</sup>, Marco Binder<sup>1,§</sup>

5

6

7 <sup>1</sup>Research Group "Dynamics of Early Viral Infection and the Innate Antiviral Response", Division  
8 Virus-Associated Carcinogenesis (F170), German Cancer Research Center, Heidelberg, Germany

9 <sup>2</sup>Department of Infectious Diseases, Molecular Virology, Centre for Integrative Infectious Disease  
10 Research, Heidelberg University, Heidelberg, Germany

11 <sup>3</sup>Faculty of Biosciences, Heidelberg University, Heidelberg, Germany

12

13 <sup>§</sup>Corresponding author: [m.binder@dkfz.de](mailto:m.binder@dkfz.de)

14

## 15 **Abstract**

16 Properly responding to DNA damage is vital for eukaryotic cells, including the induction of DNA repair,  
17 growth arrest and, as a last resort to prevent neoplastic transformation, cell death. Besides being crucial  
18 for ensuring homeostasis, the same pathways and mechanisms are at the basis of chemoradiotherapy in  
19 cancer treatment, which involves therapeutic induction of DNA damage by chemical or physical  
20 (radiological) measures. Apart from typical DNA damage response mediators, the relevance of cell-  
21 intrinsic antiviral signaling pathways in response to DNA breaks has recently emerged. Originally  
22 known for combatting viruses via expression of antiviral factors including IFNs and establishing of an  
23 antiviral state, RIG-I-like receptors (RLRs) were found to be critical for adequate induction of cell death  
24 upon the introduction of DNA double-strand breaks. We here show that presence of IRF3 is crucial in  
25 this process, most likely through direct activation of pro-apoptotic factors rather than transcriptional  
26 induction of canonical downstream components, such as IFNs. Investigating genes reported to be  
27 involved in both DNA damage response and antiviral signaling, we demonstrate that IRF1 is an  
28 obligatory factor for DNA damage-induced cell death. Interestingly, its regulation does *not* require  
29 activation of RLR signaling, but rather sensing of DNA double strand breaks by ATM and ATR. Hence,  
30 even though independently regulated, both RLR signaling and IRF1 are essential for proper  
31 induction/execution of intrinsic apoptosis. Our results not only support more broadly developing IRF1  
32 as a biomarker predictive for the effectiveness of chemoradiotherapy, but also suggest investigating a  
33 combined pharmacological stimulation of RLR and IRF1 signaling as a potential adjuvant regimen in  
34 tumor therapy.

## 35 **Introduction**

36 DNA damage is a ubiquitous and existential threat to organisms. Potential causes comprise ionizing  
37 radiation (IR), genotoxic chemicals, but also cell-intrinsic mechanisms. Among various possible DNA  
38 alterations, the most drastic and impactful are DNA double-strand breaks (DSBs). Complex  
39 mechanisms involving detection by ATM, ATR, and downstream processes including the tumor  
40 suppressor p53 and checkpoint inhibition, either lead to sufficient repair of the damage or to induction  
41 of programmed cell death [1, 2]. The latter mostly comprises apoptosis, but other forms such as  
42 necroptosis and pyroptosis have recently been reported as well. Mutations of the central DSB sensors  
43 can cause severe diseases such as ataxia telangiectasia, associated with carcinogenesis and serious  
44 immunodeficiency [3-5]. Originally discovered and best-studied in the context of the antiviral innate  
45 immune response, IRF1 has been implicated in the DNA damage response and tumor suppressor  
46 functions [6-9].

47 Following the IRF1 example, it became apparent that cell-intrinsic antiviral signaling pathways also  
48 substantially contribute to DNA damage-induced cell death. Both STING and RIG-I-like receptor  
49 (RLR) pathways detect damage-associated molecular patterns (DAMPs), such as endogenous DNA  
50 fragments and nuclear RNA, and can trigger cell death [10, 11]. Previously, RIG-I stimulation has been

51 shown to induce death of breast cancer cells, putting forward a potential application in tumor therapy  
52 [12]. Typically, the RLRs, RIG-I and MDA5, are stimulated by non-self RNA in the event of viral  
53 infection. Interaction with their adaptor MAVS leads to activation of the transcription factors IRF3, NF-  
54  $\kappa$ B p65/RELA and p50/NF $\kappa$ B1. The resulting expression of ISGs and IFNs of type I/III causes the  
55 establishment of an antiviral state and, in most cases, effective containment of the invading pathogen.  
56 In addition to apoptosis sensitizing effects of NF- $\kappa$ B and IFNs through expression of pro-apoptotic  
57 factors, direct cell death mediating effects have recently been reported for MAVS and IRF3 [13, 14].  
58 Chattopadhyay et al. were first to identify and characterize the RLR-induced IRF3-mediated pathway  
59 of apoptosis (RIPA) [15]. Stimulation of RLRs with dsRNA or viral infection induces MAVS-  
60 dependent ubiquitination of IRF3 and subsequent activation of pro-apoptotic factors independent of  
61 IRF3's transcriptional activity [16]. Furthermore, MAVS was shown to directly interact with  
62 procaspase-8, forming so-called MAVS-death-inducing signaling complexes upon viral infection [17].  
63 Here we show that RLR signaling, IRF1, and canonical DNA damage response pathways, comprising  
64 ATM/ATR and p53, are essential for efficient induction of apoptosis. We show that these pathways  
65 have independent pro-apoptotic capacities, and we present new insights into IRF1's complex cellular  
66 functions.

## 67 **Methods**

68 **Cell culture, cell line generation, and stimulation.** Cell lines were grown at 37 °C, 95 % humidity,  
69 and 5 % CO<sub>2</sub> in Dulbecco's modified eagle medium (DMEM high glucose, Life Technologies,  
70 Carlsbad, CA, USA), supplemented with final 10 % (v/v) fetal calf serum (FCS, Thermo Fisher  
71 Scientific, Waltham, MA, USA), 1x non-essential amino acids (Thermo Fisher Scientific), and  
72 100 U/ml penicillin and 100 ng/ml streptomycin (LifeTechnologies). For generation of transgene  
73 expressing A549 cell lines by lentiviral transduction, lentiviral particles were produced by transfecting  
74 HEK 293T cells with plasmids pCMV-dr8.91, pMD2.G, and the respective retroviral vector (pWPI)  
75 using calcium phosphate transfection (CalPhos Mammalian Transfection Kit, Takara Bio Europe, Saint-  
76 Germain-en-Laye, France). After two days the supernatant was harvested, sterile filtered, and used to  
77 transduce target cells two times for 24 h. Transduced cells were selected with antibiotics appropriate  
78 for the encoded resistance gene (5  $\mu$ g/ml blasticidin, MP Biomedicals, Santa Ana, CA, USA; 1  $\mu$ g/ml  
79 puromycin, Sigma Aldrich; 1 mg/ml geneticin (G418), Santa Cruz, Dallas, TX, USA). Knockout (KO)  
80 cell lines were generated by clustered regularly interspaced short palindromic repeats (CRISPR)/Cas9  
81 technology. DNA oligonucleotides coding for guideRNAs against the respective genes (sequences  
82 shown in Supplementary Table S1) were cloned into the expression vector LentiCRISPRv2 (Feng  
83 Zhang, Addgene #52961).  
84 Transduced A549 wild-type cells were selected with puromycin, single cell clones were isolated, and  
85 KO was validated by immunoblotting and functional tests (Fig. S5). A549 *IFNARI*<sup>-/-</sup> *IFNLR1*<sup>-/-</sup> *IFNGR*<sup>-/-</sup>  
86 <sup>-/-</sup> (IFNR TKO), *IRF1*<sup>-/-</sup>, *IRF1* OE, *IRF3*<sup>-/-</sup>, IRF3-eGFP H2B-mCherry, *MAVS*<sup>-/-</sup>, *MYD88*<sup>-/-</sup>, *RELA*<sup>-/-</sup>, and

87 *RIG-I*<sup>-/-</sup> were reported previously [18-22]. A549 *RIG-I* OE cells were generated by stable lentiviral  
88 transduction as described previously [19]. Cells transduced with non-targeting gRNA (sequence taken  
89 from the GeCKO CRISPR v2 library) were used as controls. PH5CH non-neoplastic hepatocytes and  
90 HepG2 cells were kindly provided by Dr. Volker Lohmann (Heidelberg University, Heidelberg,  
91 Germany). Huh7.5 cells were generously provided by Dr. Charles Rice (Rockefeller University, New  
92 York).

93 Stimulation was performed with doxorubicin (DOX, Hölzel Diagnostika, Cologne, Germany),  
94 etoposide (ETO, Cell Signaling Technology, Danvers, MA, USA), or cells were transfected with *in*  
95 *vitro* transcribed and chromatographically purified 200 bp 5'ppp-dsRNA [23], poly(C) (Sigma-  
96 Aldrich), and poly(I:C) (Sigma-Aldrich) using Lipofectamine 2000 (Invitrogen, Carlsbad, CA, USA)  
97 following the manufacturer's protocol. Cells were  $\gamma$ -irradiated with doses of 0-30 Gy using a  
98 Gammacell 40 Exactor (Best Theratronics, Ottawa, Canada).

99 **Real-time imaging of cell death.** A549 cells stably expressing histone H2B mCherry [21] were seeded  
100 at density of  $2 \times 10^3$  cells per 96-well. The next day, cells were stimulated with 1-2  $\mu$ M DOX (10 h),  
101 25  $\mu$ M ETO (10 h), 0.1 ng/ml dsRNA (8 h), or  $\gamma$ -IR. DMSO (Carl Roth, Karlsruhe, Germany), poly(C),  
102 and mock irradiation were used as appropriate controls. Post treatment, fresh medium was  
103 supplemented with 1:10 000 IncuCyte<sup>®</sup> Cytotox Green Reagent (Sartorius, Göttingen, Germany) to  
104 determine dead cells. Total cell number and dead cells were monitored every 2 h using a 10x  
105 magnification in an IncuCyte<sup>®</sup> S3 Live-Cell Analysis System (Satorius, Göttingen, Germany). For IFN  
106 pre-stimulation, 200 IU/ml IFN- $\beta$  (IFN- $\beta$ 1, Bioferon, Laupheim, Germany) or IFN- $\gamma$  (R&D Systems,  
107 Minneapolis, MN, USA) were added at the time of seeding. For inhibitor administration, 40  $\mu$ M Z-  
108 VAD-FMK (Z-VAD, R&D Systems) and 10  $\mu$ M Necrostatin-7 (Nec-7, Sigma Aldrich), or 25  $\mu$ M  
109 TPCA-1 (Sigma Aldrich) were added 2 h prior treatment. IncuCyte<sup>®</sup> Software (2019B Rev2, Sartorius,  
110 Göttingen, Germany) was used to mask cells in phase contrast images. Calculations were performed  
111 applying the following settings: red fluorescence: segmentation top-hat, radius 100  $\mu$ M, threshold  
112 (GCU) 0.4, edge split sensitivity -35, area 60-1000  $\mu$ m<sup>2</sup>, integrated intensity  $\geq 60$ ; green fluorescence:  
113 segmentation top-hat, radius 100  $\mu$ M, threshold (GCU) 10, edge split sensitivity -40, area 100-700  $\mu$ m<sup>2</sup>,  
114 eccentricity  $\leq 0.8$ , mean intensity 7-1000, integrated intensity  $\geq 2500$ . Percentage of dead cells was  
115 calculated relative to total cell count. Data represent the results of at least three biologically independent  
116 experiments. For curve charts, results were normalized to the control cell line of each replicate. Bars  
117 represent non-normalized means 36 h post treatment.

118 **Immunofluorescence microscopy and determination of cellular IRF3 distribution.** Fluorescence  
119 microscopy was performed to visualize phosphorylated histone H2A.X. After 4 h treatment with 2  $\mu$ M  
120 DOX or DMSO, or 1 h post  $\gamma$ -IR with 20 Gy or 0 Gy, cells were permeabilized with -20 °C methanol  
121 and fixed with 4 % paraformaldehyde. To block non-specific background, cells were incubated with  
122 1 % (w/v) bovine serum albumin (BSA) and 10 % (v/v) FCS for 30 min. Primary antibodies specific  
123 for phospho-H2A.X (Cell Signaling Technology, 9718, 1:1000) were applied at 4 °C over-night. Slides

124 were incubated with Alexa Fluor<sup>®</sup> 488 anti-rabbit (ThermoFisher Scientific, Waltham, MA, USA,  
125 A11008, 1:1000) and DAPI (ThermoFisher Scientific, D1306, 1:5000) for 1 h. For determination of  
126 cellular IRF3 distribution, A549 cells stably expressing IRF3-eGFP and histone H2B-mCherry were  
127 stimulated either with DOX or poly(I:C) for 12 h. Fluorescence was visualized using a Primovert  
128 microscope (Carl Zeiss, Jena, Germany).

129 **Immunoblotting.** Stimulated cells were lysed in Laemmli sample buffer, and digested with Benzonase<sup>®</sup>  
130 Nuclease (Merck Millipore, Burlington, MA, USA). For inhibitor administration, 20  $\mu$ M KU-55933  
131 (Sigma-Aldrich), 25  $\mu$ M Rabusertib (Hölzel Diagnostika), 25  $\mu$ M TPCA-1 (Sigma Aldrich), or 10  $\mu$ M  
132 VE-822 (Hölzel Diagnostika) were added 2 h prior treatment. For stimulation with IFNs, 200 IU/ml  
133 IFN- $\alpha$  (PBL Assay Science, Piscataway, NJ, USA), IFN- $\beta$ , or IFN- $\gamma$  were applied over-night. Lysed  
134 samples were further denatured at 95 °C for 5 min and cleared from detritus. Resulting protein extracts  
135 were subjected to 10 % (w/v) SDS-polyacrylamide gel electrophoresis and transferred to PVDF  
136 membranes (Bio-Rad, Hercules, CA, USA, 0.2  $\mu$ m pore size). Upon incubation with 5 % (w/v) BSA  
137 for 2 h to block non-specific background, membranes were probed using antibodies specific for  $\beta$ -actin  
138 (Sigma-Aldrich, A5441, 1:5000), calnexin (Enzo Biochem, Farmingdale, NY, USA, ADI-SPA-865-F,  
139 1:1000), CASP3 (Cell Signaling Technology, 9662S, 1:1000), CASP9 (Cell Signaling Technology,  
140 9508, 1:1000), IRF1 (Cell Signaling Technology, 8478S, 1:1000), phospho-IRF3 (pS396,  
141 ThermoFisher Scientific, MA5-14947, 1:1000), JAK1 (Cell Signaling Technology, 3332S, 1:1000),  
142 MDA5 (Enzo Biochem, ALX-210-935, 1:1000), NFKB1 (p50) (Abcam, Cambridge, UK, ab32360,  
143 1:1000), p53 (Santa Cruz Biotechnology, Dallas, TX, USA, sc-126, 1:1000), or STAT1 (BD  
144 Biosciences, Franklin Lakes, NJ, USA, 610115, 1:1000) at 4 °C over-night. For detection, anti-rabbit  
145 horseradish peroxidase (HRP) (Sigma-Aldrich, A6154-5X1ML, 1:20 000) or anti-mouse HRP (Sigma-  
146 Aldrich, A4416-5X1ML, 1:10 000) were applied for 1 h, membranes were covered with Amersham  
147 ECL Prime Western Blotting Detection Reagent (ThermoFisher Scientific) for 1 min, and luminescence  
148 was detected using a sensitive CCD camera system (ECL ChemoCam Imager 3.2, INTAS Science  
149 Imaging Instruments, Göttingen, Germany). Densitometric analysis of the protein bands was performed  
150 using ImageJ (1.52e). Data shown represent the results of at least three biologically independent  
151 experiments.

152 **Quantitative PCR with reverse transcription (qRT-PCR).** Upon stimulation, cells were lysed and  
153 total RNA was isolated with the Monarch RNA isolation kit (New England Biolabs, Ipswich, MA,  
154 USA), following the manufacturer's protocol. After extraction, complementary DNA (cDNA) was  
155 generated using the High Capacity cDNA Reverse Transcription kit (ThermoFisher Scientific).  
156 Determination of messenger RNA (mRNA) expression was performed using iTaq Universal SYBR<sup>®</sup>  
157 Green Supermix (Bio-Rad) on a CFX96 real-time-system (Bio-Rad). Sequences of specific exon-  
158 spanning PCR primers are shown in Supplementary Table S2. GAPDH mRNA was used as a  
159 housekeeping gene control and relative expression determined by  $2^{\Delta Ct}$  (thus, not normalizing to  
160 reference condition).

161 **Cell Viability.** A549 cells were seeded at a density of  $6 \times 10^3$  cells per 96-well. Upon treatment with  
162 2  $\mu$ M DOX or DMSO for 24 h, cell viability was determined using the CellTiter-Glo<sup>®</sup> luminescent cell  
163 viability assay (Promega, Madison, WI, USA) following the manufacturer's protocol. Luciferase  
164 activity was measured using a Mithras LB 943 multimode reader (Berthold Technologies, Bad Wildbad,  
165 Germany).

166 **Caspase activity.** A549 cells were seeded at density of  $6 \times 10^3$  cells per 96-well. 48 h post treatment  
167 with 0-2  $\mu$ M DOX for 10 h, caspase-3/7 activity was determined using the Apo-ONE<sup>®</sup> homogeneous  
168 caspase-3/7 assay (Promega) following the manufacturer's instructions. Resulting fluorescence was  
169 measured using the Mithras LB 943 multimode reader (Berthold Technologies).

#### 170 **Statistics**

171 Comparison of datasets was performed using a paired, two-tailed Student's t-test. \* indicates  $p \leq 0.05$ ,  
172 \*\*  $p \leq 0.01$ , \*\*\*  $p \leq 0.001$ , \*\*\*\*  $p \leq 0.0001$ . Error bars represent standard deviation.

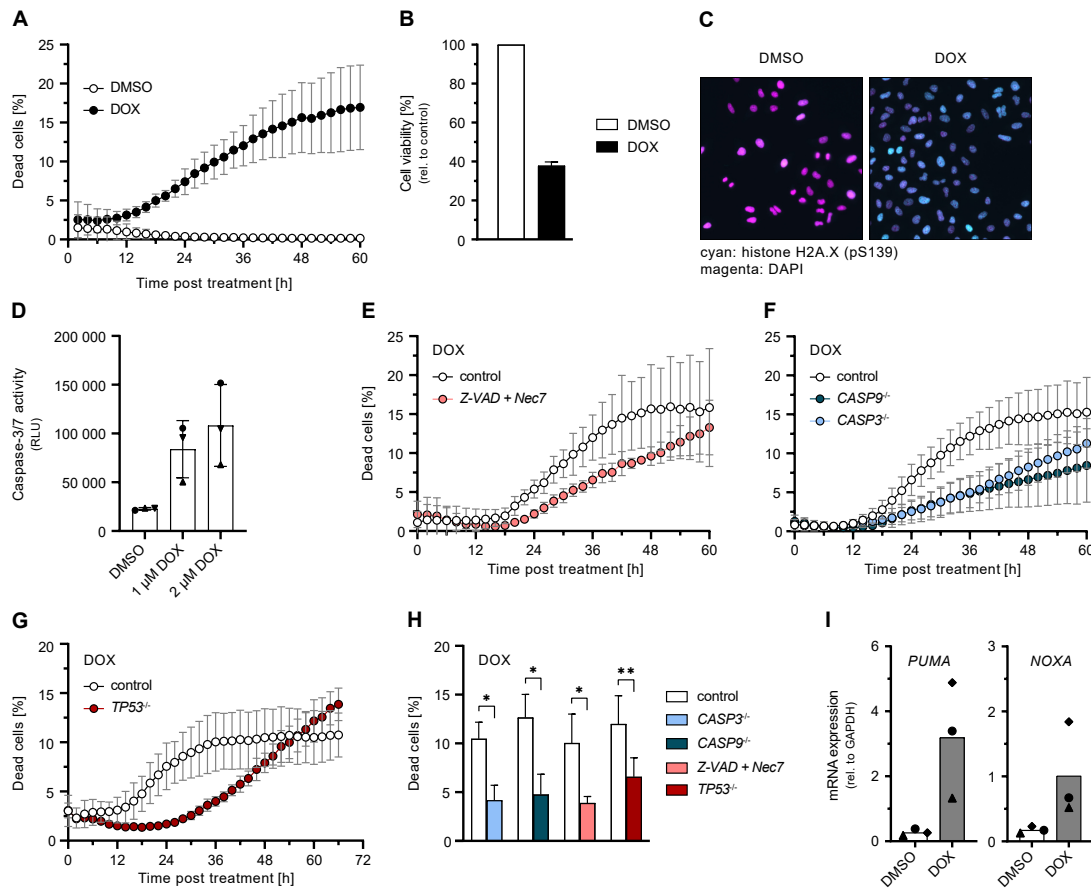
## 173 **Results**

### 174 **Apoptosis induction via DNA damage response pathway in A549 cells**

175 To investigate the molecular links between DNA damage-induced cell death and innate immune  
176 signaling, we used immunocompetent A549 human lung carcinoma cell lines with functional knockouts  
177 (KOs) of components of both pathways. Cells were treated with DNA DSB inducers, specifically  $\gamma$ -IR  
178 or the topoisomerase II inhibitors doxorubicin (DOX) and etoposide (ETO), and the resulting cell death  
179 was monitored on single-cell level by real-time imaging.

180 Treatment of A549 cells with DOX resulted in pronounced cell death (Fig. 1A) and a corresponding  
181 reduction of bulk cell viability (Fig. 1B), accompanied by the detection of the DNA damage marker  
182 phospho-histone H2A.X by immunofluorescence (Fig. 1C). As in DMSO control conditions no cell  
183 death was observed (Fig. 1A), for the clarity of presentation we omitted this control in the following  
184 figures (data was acquired in every experiment). In order to characterize the type of cell death  
185 predominant upon DOX-induced DNA damage, we first evaluated activation of caspase-3 and -7 being  
186 pivotal markers of apoptosis. DOX treatment activated caspase-3 and -7 in a dose-dependent manner  
187 (Fig. 1D). Conversely, we treated cells with the pan-caspase inhibitor Z-VAD, or depleted caspase-3 or  
188 -9. Both approaches resulted in a significant reduction of cell death upon DOX treatment (Fig. 1E, F,  
189 H). These findings confirmed prior reports that cell death driven by DOX is mainly due to apoptosis  
190 [24]. Next, we investigated typical components of the DNA damage response upstream of caspase  
191 activation. In line with p53's (*TP53*) essential role in inducing apoptosis, depletion of p53 showed a  
192 significant reduction of cell death (Fig. 1G, H). Interestingly, *TP53*<sup>-/-</sup> had the opposite effects at late  
193 time points, elevating cell death for time points >54 h (Fig. 1G). Amongst others, p53 induces apoptosis  
194 via activation of PUMA and NOXA. Accordingly, we found *PUMA* and *NOXA* transcript levels to be  
195 increased in DOX treated cells (Fig. 1I), supporting a canonical DNA damage response through p53 in  
196 DOX-treated A549 cells.





197

198 **Fig. 1. Induction of apoptosis upon DOX-mediated DNA damage.**

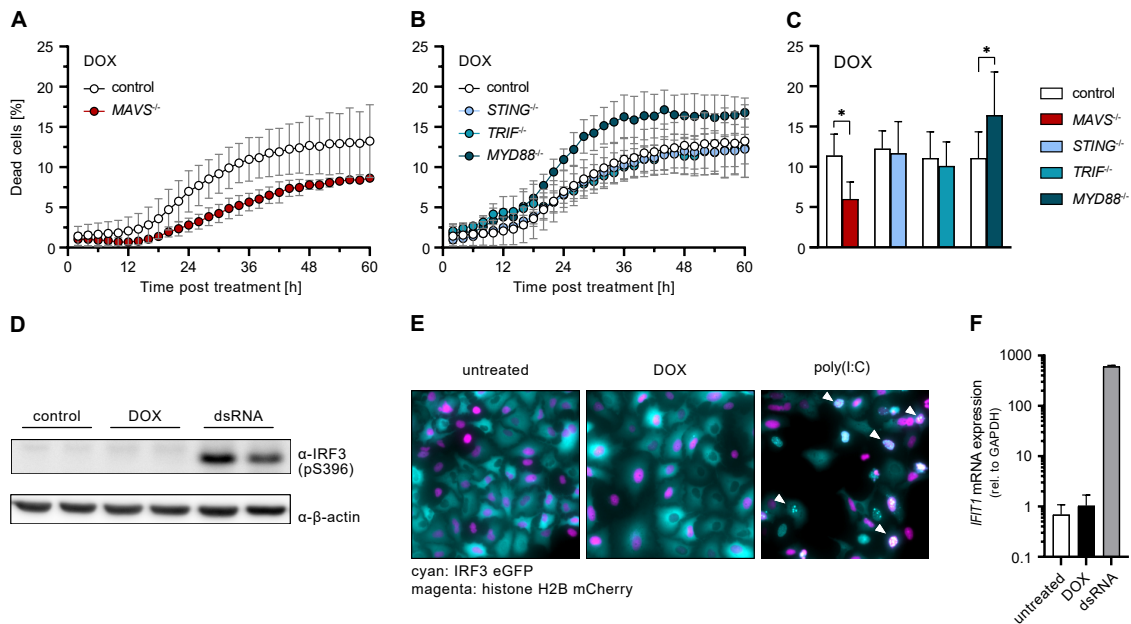
199 (A) Percentage of dead A549 cells relative to total cells counted over time post DOX or DMSO treatment. (B)  
 200 Cell viability of A549 cells post DOX treatment for 24 h. (C) Immunofluorescence of phosphorylated histone  
 201 H2A.X (S139) (cyan) and DAPI-stained nuclei (magenta) in A549 cells post DOX treatment for 4 h. (D) Caspase-  
 202 3/7 activity of A549 cells 24 h post DOX treatment for 10 h. (E-H) Percentage of dead A549 cells with caspase  
 203 inhibition or functional KO of the indicated genes relative to total cells counted over time (E-G) or 36 h (H) post  
 204 DOX treatment. (I) A549 cells were treated with 1  $\mu$ M DOX or DMSO for 24 h. PUMA and NOXA mRNA  
 205 transcripts were determined by qRT-PCR. (A, B, D-I) Data shown represent the results of at least three  
 206 biologically independent experiments.

207

### 208 **Relevance of innate antiviral immunity pathways in DNA damage induced cell death**

209 In order to investigate the contribution of antiviral signaling cascades to the induction of DSB-induced  
 210 cell death, we compared the impact of the major antiviral pathways using KOs of their respective  
 211 signaling adapters. We observed DOX-induced cell death to be significantly reduced only by MAVS  
 212 depletion (RLR signaling), but not so in the absence of STING (cGAS signaling), TRIF (TLR3  
 213 signaling), or MYD88 (general TLR signaling) (Fig. 2A-C). Despite RLR signaling appeared to play a  
 214 major role, neither canonical IRF3 phosphorylation nor its nuclear translocation could be detected

215 (Fig. 2D, E). Consistently, there was also no characteristic RLR-mediated induction of ISGs, such as  
 216 *IFIT1* (Fig. 2F).



217  
 218 **Fig. 2. Relevance of antiviral signaling adapters and ISG response during DOX-induced DNA damage**  
 219 **response.**

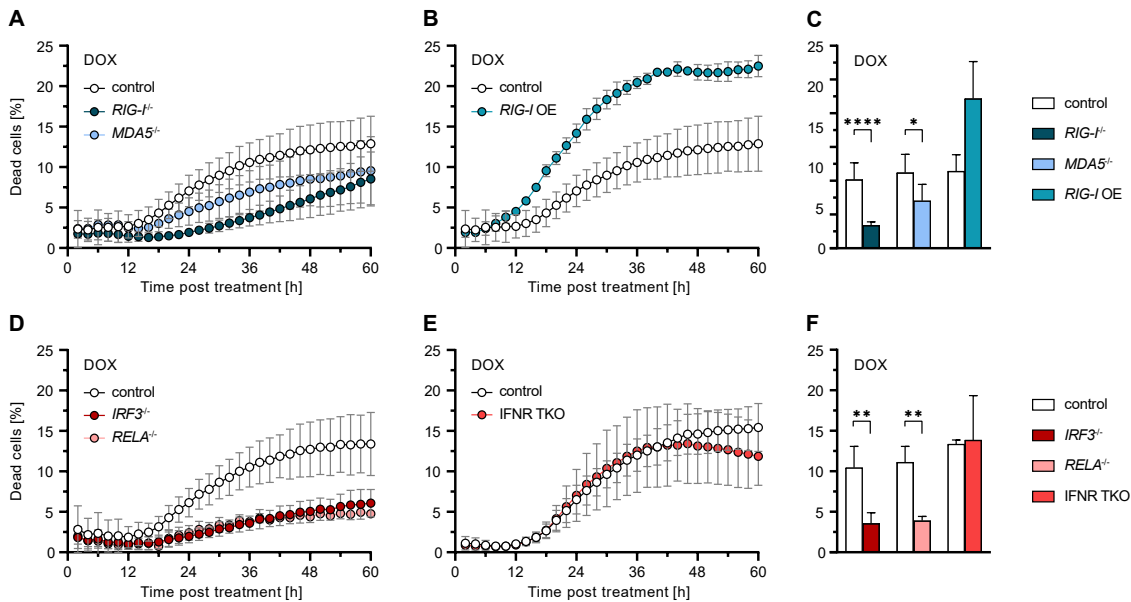
220 (A-C) Percentage of dead A549 cells with functional KO of the indicated genes relative to total cells counted over  
 221 time (A, B) or 36 h (C) post DOX treatment. (D) A549 cells were stimulated with 1  $\mu$ M DOX or 1 ng/ml dsRNA  
 222 for 8 h. Phosphorylated IRF3 (S396) was determined by western blot. (E) A549 cells were stimulated with 1  $\mu$ M  
 223 DOX or 2  $\mu$ g/ml poly(I:C) for 12 h. Cellular distribution of IRF3 eGFP (cyan) and histone H2B (magenta) was  
 224 visualized by immunofluorescence microscopy. (F) A549 cells were stimulated with 1  $\mu$ M DOX or 10 ng/ml  
 225 dsRNA for 24 h. *IFIT1* mRNA transcripts were determined by qRT-PCR. (A-C, F) Data shown represent the  
 226 results of at least three biologically independent experiments.

227  
 228 Given the observed relevance of MAVS in DOX-induced cell death, we further analysed the effect of  
 229 specific RLR depletion. Both *RIG-I*<sup>-/-</sup> and *MDA5*<sup>-/-</sup> reduced cell death upon DOX treatment, however,  
 230 *RIG-I* exhibited a considerably stronger effect (Fig. 3A, C). Reciprocally, *RIG-I* overexpression (OE)  
 231 markedly increased cell death upon DOX treatment (but not in untreated conditions, compare Fig. S1A),  
 232 underlining the decisive role of RLR signaling in this process (Fig. 3B, C). In order to determine the  
 233 factors responsible for mediating cell death downstream of MAVS, we further examined the influence  
 234 of transcription factors IRF3 and NF- $\kappa$ B p65/RELA. We observed that depletion of either factor  
 235 significantly reduced DOX-induced cell death (Figure 3D, F). Using IFN-“blind” A549 *IFNARI*<sup>-/-</sup>  
 236 *IFNLRI*<sup>-/-</sup> *IFNGR*<sup>-/-</sup> (IFNR TKO) cells, we demonstrated that this effect was independent of a response  
 237 mediated by secreted IFNs (Fig. 3E, F), which was further confirmed using *STAT1*<sup>-/-</sup> cells (Fig. S1B).  
 238 This was in accordance with the lack of ISG expression observed previously (Fig. 2F). Thus, IRF3



239 appears to have death sensitizing effects distinct from its classical transcriptional activity in the antiviral  
240 program.

241 Taken together, we demonstrated that RLR signaling is required for the induction of cell death after  
242 DNA damage and that this function is independent of IFN secretion and the induction of canonical  
243 ISGs.



244  
245 **Fig. 3. Implications of RLR signaling components and IFN signaling on DOX-induced apoptosis.**  
246 (A-F) Percentage of dead A549 cells with functional KO or OE of the indicated genes relative to total cells counted  
247 over time (A, B, D, E) or 36 h (C, F) post DOX treatment. Data shown represent the results of at least three  
248 biologically independent experiments.

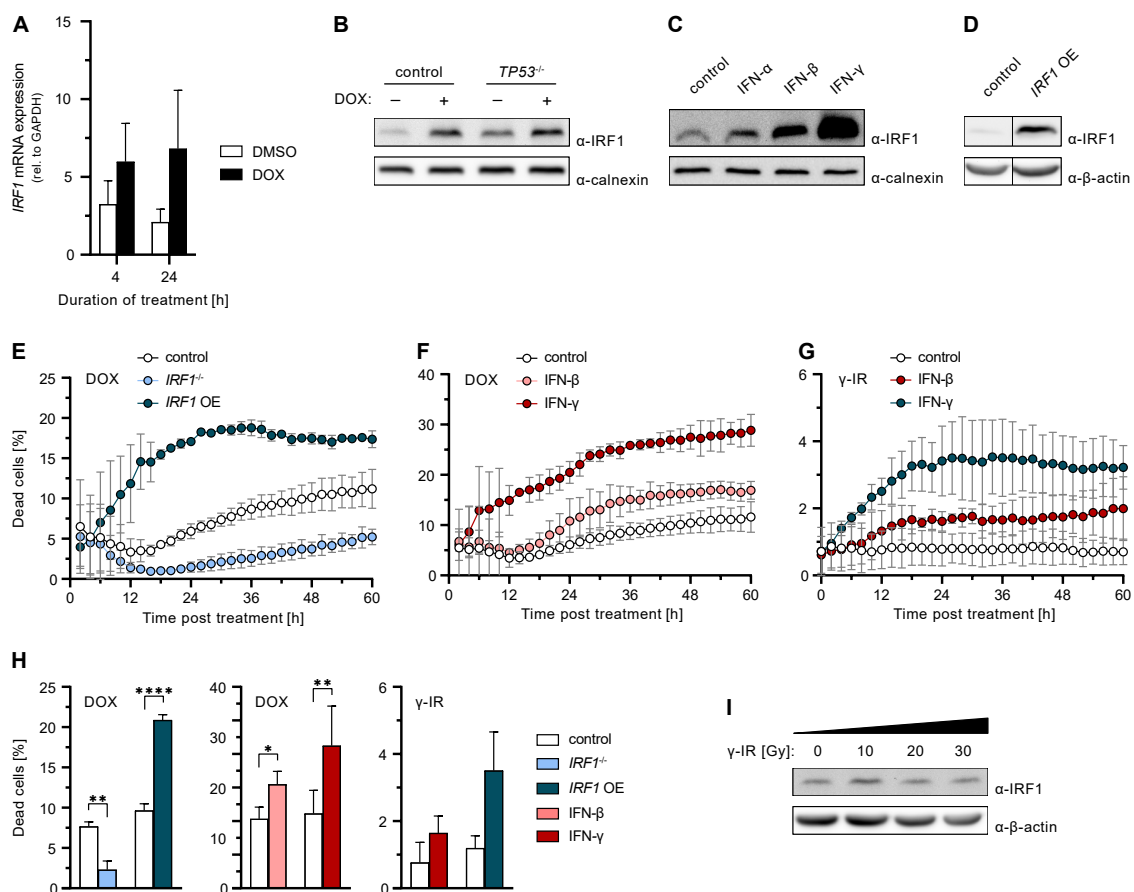
### 249 250 **Role of IRF1 in DNA damage induced apoptosis**

251 Another transcription factor of the IRF family important for antiviral defenses [6, 18], IRF1, has  
252 previously also been implicated with the DNA damage response [25]. We hypothesized that upon  
253 genotoxic insult, IRF1 might be a downstream target of the RLR/IRF3 pathway, as reported for virus  
254 infection, and thereby link RLR activity to the DNA damage response. Indeed, upon DOX treatment,  
255 we observed IRF1 upregulation at the mRNA (Fig. 4A) and protein level (Fig. 4B). Of note, *IRF1*  
256 induction occurred independently of the presence of p53 (Fig. 4B). In order to determine the relevance  
257 of IRF1 to cell death, we next tested *IRF1*<sup>-/-</sup> cells in DOX treatment. Strikingly, IRF1 depletion almost  
258 completely abolished DOX-induced cell death (Fig. 4E, H). Conversely, increasing IRF1 abundance,  
259 either by OE through stable transduction or by pre-stimulation of cells with IFN- $\beta$  or IFN- $\gamma$ , markedly  
260 increased cell death upon DOX treatment (Fig. 4E, F, H), and the percentage of dead cells correlated  
261 with IRF1 levels in western blot (Fig. 4C, D). Notably, neither IFN stimulation alone, nor DOX  
262 treatment in IFN-primed but IRF1-depleted cells did induce cell death (Fig. S2A, B). Surprisingly, the  
263 same phenotype was observed in *RIG-I*<sup>-/-</sup> conditions (Fig. S2C), in which IRF1 was present, suggesting

264 a strict requirement of both RLR signaling and *IRF1* induction for proper triggering and/or execution  
 265 of apoptosis. Similar observations were also made after ETO treatment (Fig. S2D, E), ruling out DOX-  
 266 specific effects.

267 The fundamental importance of IRF1 was additionally demonstrated in response to  $\gamma$ -IR. Although  
 268 irradiation did induce DNA damage in A549 cells (Fig. S2F), we could neither observe induction of  
 269 *IRF1* expression nor any cell death upon administration of up to 30 Gy (Fig. 4G-I). Strikingly, induction  
 270 of cell death upon  $\gamma$ -IR was restored under conditions of elevated IRF1 levels, such as stable OE or  
 271 IFN- $\gamma$  pre-stimulation (Fig. 4G, H). In line with this, cells in which  $\gamma$ -IR naturally leads to an  
 272 upregulation of *IRF1* expression, such as PH5CH cells, did exhibit a dose-dependent induction of cell  
 273 death (Fig. S2G, H).

274 Thus, we showed that besides p53 and RLR signaling, IRF1 is essential for proper triggering of cell  
 275 death upon DNA damage. IFNs, in particular IFN- $\gamma$ , sensitize cells for DNA damage-induced apoptosis  
 276 through upregulation of IRF1.



277  
 278 **Fig. 4. Relevance of IRF1 on DNA damage-induced cell death.**

279 (A) A549 cells were treated with 1  $\mu$ M DOX or DMSO for 10 h. IRF1 mRNA transcripts were determined by  
 280 qRT-PCR. (B) A549 cells were treated with 1  $\mu$ M DOX or DMSO for 10 h. Levels of IRF1 were determined by  
 281 western blot. (C) A549 cells were stimulated with IFN- $\alpha$ , IFN- $\beta$ , or IFN- $\gamma$  over-night. Levels of IRF1 were  
 282 determined by western blot. (D) Levels of IRF1 in A549 control and *IRF1* OE cells were determined by western

283 blot. **(E-H)** Percentage of dead A549 cells with functional KO or OE of IRF1, or post IFN pre-stimulation relative  
284 to total cells counted over time **(E-G)** or 36 h **(H)** post DOX or  $\gamma$ -IR (20 Gy) treatment. **(I)** A549 cells were  $\gamma$ -  
285 irradiated. After 10 h IRF1 protein levels were determined by western blot. **(A, E-H)** Data shown represent the  
286 results of at least three biologically independent experiments.

287

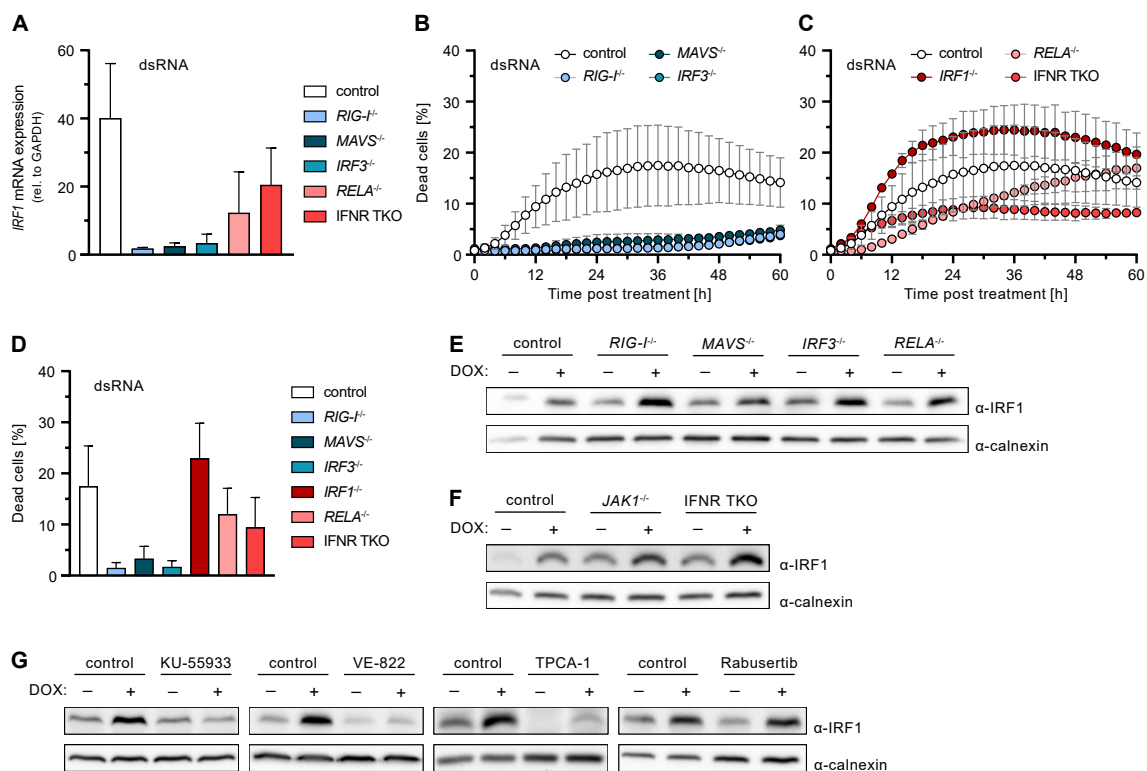
### 288 **Regulation of *IRF1* expression upon DNA damage**

289 Above we have shown that RLR/IRF3 signaling as well as expression of *IRF1* are crucially important  
290 for DNA damage-induced cell death. We further found IRF1 to be consistently induced under all tested  
291 conditions of DNA damage leading to cell death. We now aimed to confirm whether IRF1 is in fact  
292 induced as a downstream target of RLR signaling. We first investigated the induction of *IRF1*  
293 expression after RIG-I stimulation using dsRNA as a canonical, highly specific agonist [23]. Indeed,  
294 we observed a fully RLR-dependent (RIG-I, MAVS, IRF3) increase of IRF1 levels, with a partial  
295 contribution of p65/RELA and IFN signaling (IFNR TKO) (Fig. 5A), in line with a recent report of our  
296 lab [18]. dsRNA-stimulation furthermore also led to the induction of cell death, which was fully  
297 abolished upon depletion of the RLR signaling components RIG-I, MAVS, or IRF3 (Fig. 5B, D).  
298 Depletion of p65/RELA and the IFN receptors (IFNR TKO) had minor pro-survival effects, suggesting  
299 a major role for transcription-independent RIPA with a possible but limited role for IFN signaling and  
300 ISG induction (Fig. 5C, D). Interestingly and in clear contrast to the situation upon DNA damage,  
301 dsRNA-induced cell death was independent of IRF1 (Fig. 5C). Nonetheless, experimentally elevating  
302 IRF1 levels markedly increased the percentage of dead cells also in this setting (Fig. S3A, B).

303 These findings confirmed that, despite not being essential for cell death induction, IRF1 is induced  
304 downstream of RLR signaling, at least when stimulated by a strong RIG-I specific agonist. We next  
305 investigated whether this would be also the case in the context of DNA damage. Unexpectedly, upon  
306 treatment of cells with DOX, induction of *IRF1* expression was neither affected by depletion of RLR  
307 nor of IFN signaling components, including JAK1 (Fig. 5E, F; Fig. S3C). This suggested *IRF1*  
308 expression is induced independently of and coincidentally with antiviral RLR signaling upon DNA  
309 damage. We therefore hypothesized sensing of DNA damage might directly induce *IRF1*. To test this,  
310 we treated cells with specific inhibitors of the prototypical DSB sensors ATM and ATR, as well as  
311 potential downstream pathways. We found *IRF1* induction upon DOX-treatment to be completely  
312 blocked by the ATM inhibitor KU-55933 [26] and the ATR inhibitor VE-822 [27], suggesting important  
313 roles of these sensors in activation of IRF1 (Fig. 5G; Fig. S3D).

314 As *IRF1* expression has previously been shown to be NF- $\kappa$ B sensitive [28], we employed the common  
315 pan-NF- $\kappa$ B and JAK1 inhibitor TPCA-1 [29, 30]. Remarkably, TPCA-1 treatment completely  
316 prevented the induction of *IRF1* expression upon DOX treatment, and even strongly diminished basal  
317 expression (Fig. 5G, Fig. S3D). This effect could further be confirmed upon RLR-stimulation with  
318 dsRNA (Fig. S4A) and even upon IFN- $\gamma$  treatment, which is a strong and well-studied canonical inducer  
319 of *IRF1* (Fig. S4B). We could rule out a cell line (A549) specific effect by testing three other human

320 cell lines, PH5CH, HeLa and Huh7.5 (Fig. S4C). To our knowledge, this striking effect of TPCA-1 on  
 321 *IRF1* expression has not been reported before. Again, corroborating IRF1's crucial role in DNA  
 322 damage-induced apoptosis, suppressing *IRF1* induction by TPCA-1 also reduced cell death in DOX-  
 323 treated A549, PH5CH, HeLa, and Huh7.5 cells (Fig. S4D).  
 324 Finally, we aimed to identify which signaling pathway and NF- $\kappa$ B subunit would be responsible for  
 325 *IRF1* expression upon triggering the DNA damage response. As reported in literature, ATR may signal  
 326 through CHK1 to activate p50/NFKB1, a potential target of TPCA-1 [31, 32]. We therefore inhibited  
 327 CHK1 by Rabusertib [33] prior to DOX-treatment. However, our experiments did not reveal any effect  
 328 of CHK1 inhibition or p50/NFKB1 depletion on IRF1 levels (Fig. 5G; Fig. S3D, E). We hence conclude  
 329 that a so far elusive pathway downstream of the ATM/ATR system induces *IRF1*.  
 330 Taken together, we demonstrated that *IRF1* expression upon DOX-treatment is induced by the DSB  
 331 sensors ATM/ATR rather than RLR signaling. This induction is independent of CHK1 signaling.  
 332 Additionally, we identified a previously unappreciated IRF1-depleting effect of the NF- $\kappa$ B inhibitor  
 333 TPCA-1.



334  
 335 **Fig. 5. Effect of cell-intrinsic antiviral signaling components on dsRNA-induced cell death and *IRF1***  
 336 **expression.**  
 337 (A) A549 cells with functional KO of the indicated genes were stimulated with 2 ng/ml dsRNA for 6 h. IRF1  
 338 mRNA transcripts were determined by qRT-PCR. (B-D) Percentage of dead A549 cells with functional KO of the  
 339 indicated genes relative to total cells counted over time (B, C) or 36 h (D) post dsRNA stimulation. (E-G) A549  
 340 cells with functional KO of the indicated genes or administration of the indicated inhibitors were treated with

341 2  $\mu$ M DOX or DMSO for 6 h. Levels of IRF1 were determined by western blot. (A-D) Data shown represent the  
342 results of at least three biologically independent experiments.

### 343 **Discussion**

344 Cells, particularly of multicellular organisms, have elaborate systems in place ensuring the integrity of  
345 their genome, as DNA damage poses severe risks of accumulating tumorigenic mutations or alterations.  
346 In response to excessive DNA damage beyond the potential of being properly repaired, cells trigger the  
347 execution of cell death programs, most commonly apoptosis [34]. This is also exploited for common  
348 cancer chemoradiotherapies, in which excessive DNA damage is radiologically (e.g.,  $\gamma$ -IR) or  
349 pharmacologically (e.g., DOX or ETO) introduced, leading to the induction of cell death programs  
350 particularly in dividing tissues such as tumors. Elucidating the underlying mechanisms of how DNA  
351 damage molecularly leads to cell death is crucial to a better understanding of the circumstances leading  
352 to cancer and the pathways relevant for chemoradiotherapy. While classical DNA damage checkpoint  
353 control via p53 has been investigated thoroughly [1], much less is known about the relevance and  
354 contribution of non-canonical pathways. For example, a ground-breaking study surprisingly found the  
355 antiviral type I IFN pathway essential for certain chemotherapies' efficacy [35]. Cytostatic and pro-  
356 apoptotic effects of IFNs have long been noticed [36-38]; however, it remained unresolved what  
357 triggered the production of IFNs in the studied context in the first place. Recent data also revealed cell-  
358 intrinsic triggering of cell death upon activation of antiviral signaling adapters, such as MAVS and  
359 STING. Interestingly, this was not only the case for viral infections, but also in response to DNA  
360 damage [10, 11, 39].

361 In the present study, we confirm this interrelationship between DNA damage response and antiviral  
362 signaling pathways, and we demonstrate an almost complete dependence of DOX- and ETO-triggered  
363 cell death on the presence of intact RLR/MAVS signaling. In clear contrast to recently published data,  
364 other branches of the cell-intrinsic antiviral defense, such as the TLR or the cGAS/STING system [10,  
365 40, 41], did not affect DOX-induced cell death in our experimental setup. Instead, the cytosolic RNA  
366 sensors RIG-I and, to a lesser extent, MDA5 were triggered and essential for the induction of cell death.  
367 This is in line with a study by Ranoa et al. suggesting small nuclear RNAs U1 and U2 translocate into  
368 the cytoplasm in irradiated cells and trigger RIG-I activation [11]. In our experimental system, an intact  
369 RIG-I/MDA5-MAVS-IRF3 axis was essential for DNA damage induced cell death; however, we could  
370 not observe canonical transcriptional activities of IRF3, such as the induction of IFN genes or ISGs.  
371 While the relevance of both IRF3 and p65/RELA suggested the involvement of *IFNB* expression, KO  
372 of the receptors for all three types of IFNs (IFNR TKO) did not impact cell death. A plausible  
373 mechanism for this IFN-independent triggering of apoptosis is RIPA, involving LUBAC-dependent  
374 ubiquitylation of IRF3 and subsequent activation of pro-apoptotic BH3-only proteins [16]. The clear  
375 contribution of p65/RELA in our experiments might be through its transcriptional activation of further

376 pro-apoptotic proteins [42]. To our knowledge, cooperative effects between RPA and NF- $\kappa$ B have not  
377 been described before and may be an interesting subject for future investigations.

378 Efficient sensing of nuclear DSBs and triggering an appropriate response is critical for cell survival  
379 upon DNA damage, or for initiating cell death and preventing potentially cancerous transformation. As  
380 expected, we observed an essential role for p53, highlighting its central function in checkpoint control,  
381 coordinating DNA damage repair and triggering apoptosis as a last resort [43]. Interestingly, depletion  
382 of p53 reduced the number of apoptotic cells at early time points, but increased cell death at later times.  
383 Thus, absence of p53 led to a lack of induction of apoptosis in response to DOX-mediated DSBs at first,  
384 but likely massive accumulation of unrepaired DNA damage eventually led to increased, putatively  
385 necrotic cell death [44]. As a factor potentially linking the DNA damage response and antiviral  
386 signaling, we investigated the role of the multifunctional transcription factor IRF1, as it is known to be  
387 involved in both the DNA damage response [8, 25] and IFN signaling [6, 18, 45]. Indeed, we found that  
388 *IRF1* was considerably upregulated upon DOX and ETO treatment as well as  $\gamma$ -IR in different cell lines.  
389 Interestingly, only in A549 cells, described to be relatively radioresistant as a common characteristic  
390 for non-small cellular lung cancers [46], *IRF1* was not appreciably induced upon irradiation. We also  
391 observed a reduced histone H2A.X phosphorylation after  $\gamma$ -IR compared to DOX treatment, but  
392 potential underlying mechanisms are only partially understood and may comprise several processes [47,  
393 48]. Nonetheless, we could further corroborate this clear correlation between *IRF1* induction and  
394 triggering/execution of a cell death program on a functional level. Experimentally increasing IRF1  
395 levels by stable OE or by pre-treatment of cells with IFN- $\gamma$ , known as a strong inducer of *IRF1* [45],  
396 radioresistance of A549 cells could be overcome. A similar effect has previously been demonstrated in  
397 T cells [25]. In our experiments, increased *IRF1* expression also led to a sensitization towards DOX-  
398 treatment. *Vice versa*, *IRF1* KO almost completely rescued cell survival upon DOX-, ETO- and  $\gamma$ -IR-  
399 induced DNA damage. These observations clearly establish a fundamentally important role of IRF1 in  
400 DNA damage-induced cell death. This is in accordance with literature suggesting IRF1 as a biomarker  
401 for radioresistance in tumor cells [49]. For example, extremely radioresistant osteosarcomas were  
402 shown to exhibit significantly reduced *IRF1* expression levels [50]. Our data further support  
403 establishing IRF1 as a predictive biomarker in chemoradiotherapy in tumor patients.

404 Our finding strongly suggested IRF1 to be the functional link between the DNA damage response and  
405 the antiviral system, with RLR signaling (either directly or via the IFN/JAK/STAT cascade) leading to  
406 transcriptional activation of IRF1. However, KO experiments clearly refuted this hypothesis. Neither  
407 KO of essential factors of the RLR pathway nor of IFN signaling components abolished *IRF1* induction  
408 upon DNA damage, suggesting that RLR signaling may activate IRF1 post-translationally. Generally,  
409 IRF1 is thought to be only regulated on a transcriptional level [45]. However, one study reports the  
410 requirement for “licensing” of IRF1 to become fully active, which required TLR signaling and MYD88  
411 [51]. In preliminary experiments, we did not find any evidence for post-translational modifications in  
412 our setting, but this may warrant deeper investigations in the future. Alternatively, IRF1 might enhance



413 the transcriptional response of IRF3, as reported before [52]. While we cannot rule out this possibility,  
414 the virtually complete inhibition of cell death in *IRF1*<sup>-/-</sup> despite abundant presence of IRF3 makes this  
415 unlikely. In another study, we have also not found any indication of a dampening of IRF3 responses in  
416 A549 *IRF1*<sup>-/-</sup> cells [18]. Notably, despite IRF1 being critically important for cell death induction in our  
417 system, *IRF1* (over-)expression alone did not suffice to elicit apoptosis. We therefore suspect RLR  
418 signaling and IRF1 activity to cooperate further downstream, putatively via the transcriptional  
419 activation of complementary pro-apoptotic factors.

420

421 It is interesting to note that cell death is also elicited upon RLR stimulation by dsRNA (the canonical  
422 way to trigger antiviral signaling). Also in this case, *IRF1* is induced, but strictly dependent on RIG-I  
423 and to a lesser extent dependent on IFN signaling. Surprisingly, however, depletion of IRF1 did not  
424 affect the cell death rate upon dsRNA stimulation, pointing towards transcription-independent  
425 mechanisms such as RIPA [15]. Still, KO of NF- $\kappa$ B (*RELA*) or the IFN receptors (IFNR TKO) affect  
426 cell death, suggesting some transcriptional regulation, which, however, was independent of IRF1. This  
427 may suggest that full-fledged RLR signaling upon dsRNA encounter induces a sufficiently broad  
428 transcriptional response, which (in contrast to the situation upon DNA damage) itself is capable of  
429 triggering apoptosis. Strikingly, even in dsRNA stimulation, ectopic OE of *IRF1* or pre-treatment of  
430 cells with IFN- $\gamma$  led to a notable increase in the number of dying cells, putatively by the same  
431 cooperative pro-apoptotic effects observed in the case of DNA damage. This observation of a general  
432 sensitization for cell death by IRF1 is in line with data showing that *IRF1* OE enhances apoptosis in  
433 breast or gastric cancer treatment [53-55]. It is further plausible to speculate that reported pro-apoptotic  
434 effects of type I IFN [56, 57] would also be mediated by upregulation of *IRF1* through homodimeric  
435 STAT1 transcription factor complexes (GAF) inadvertently formed early upon IFNAR engagement  
436 [58]. This could mechanistically explain how IFN- $\alpha$  improved chemotherapy response and overall  
437 survival in a murine tumor model [35]. Thus, evidence further accumulates suggesting *IRF1*-inducing  
438 agents to be more broadly considered as adjuvants in tumor therapy.

439 Two central questions remain: firstly, which pro-apoptotic factors are specifically induced by IRF1  
440 upon DNA damage that so potently sensitize cells to committing suicide upon (slight) RLR triggering.  
441 To this end, we are currently investigating IRF1-dependent candidate genes induced upon DOX-  
442 treatment at a transcriptomic level. Secondly, how is *IRF1* induced upon DNA damage in the first place  
443 if not through classical STAT1:STAT1 activity. In our study, we found its transcriptional regulation to  
444 be fully independent of RLR signaling and p53 but completely reliant on DNA DSB sensing via ATM  
445 and ATR. Still, the downstream pathway leading to *IRF1* expression remains elusive. While p65/RELA  
446 or p50/NFKB1 depletion did not affect *IRF1* induction, it was completely abolished by TPCA-1, a  
447 commonly known inhibitor of NF- $\kappa$ B. Interestingly, TPCA-1 considerably reduced baseline *IRF1*  
448 expression independent of the cell line used, and could even abolish the strong induction upon IFN- $\gamma$   
449 treatment. Thus, in addition to its inhibitory effects on NF- $\kappa$ B, JAK1, and STAT3 [29, 30, 59], TPCA-

450 1 appears to specifically and very efficiently inhibit the activity of an essential transcription factor for  
451 *IRF1*.

452 In conclusion, our study highlights the critical relevance of the antiviral RLR system for the proper and  
453 timely induction of cell death upon DNA damage. We provide evidence for independent but cooperative  
454 involvement of p53, IRF1 and IRF3 activity upon detection of DNA DSBs by the ATM/ATR  
455 machinery. We show that elevating expression levels of *IRF1* lead to the sensitization towards cell death  
456 across different genotoxic insults, such as chemotherapeutics,  $\gamma$ -IR or cytosolic dsRNA (i.e. virus  
457 infection). These data corroborate a fundamental role for IRF1 and RLR signaling in DNA damage-  
458 mediated cell death and suggest future exploration of *IRF1* inducers, such as IFN- $\gamma$ , together with low-  
459 dose RIG-I agonists for their potential as highly efficacious adjuvants in chemoradiotherapy.  
460 Additionally, our findings support IRF1 as a biomarker predictive for chemo- and radio-sensitivity of  
461 tumors.

462

### 463 **Literature**

- 464 1. Sullivan, K.D., et al., *The p53 circuit board*. Biochimica et Biophysica Acta (BBA) -  
465 Reviews on Cancer, 2012. **1825**(2): p. 229-244.
- 466 2. Shiloh, Y. and Y. Ziv, *The ATM protein kinase: regulating the cellular response to*  
467 *genotoxic stress, and more*. Nature Reviews Molecular Cell Biology, 2013. **14**(4): p.  
468 197-210.
- 469 3. Shao, L., et al., *Deficiency of the DNA repair enzyme ATM in rheumatoid arthritis*.  
470 Journal of Experimental Medicine, 2009. **206**(6): p. 1435-1449.
- 471 4. Deng, X., et al., *Defective ATM-p53-mediated apoptotic pathway in multiple sclerosis*.  
472 Annals of Neurology, 2005. **58**(4): p. 577-584.
- 473 5. Hecht, F. and B.K. Hecht, *Cancer in Ataxia-telangiectasia patients*. Cancer Genetics  
474 and Cytogenetics, 1990. **46**(1): p. 9-19.
- 475 6. Fujita, T., et al., *Evidence for a nuclear factor(s), IRF-1, mediating induction and*  
476 *silencing properties to human IFN-beta gene regulatory elements*. The EMBO Journal,  
477 1988. **7**(11): p. 3397-3405.
- 478 7. Yamane, D., et al., *Basal expression of interferon regulatory factor 1 drives intrinsic*  
479 *hepatocyte resistance to multiple RNA viruses*. Nature Microbiology, 2019. **4**(7): p.  
480 1096-1104.
- 481 8. Harada, H., et al., *Anti-oncogenic and oncogenic potentials of interferon regulatory*  
482 *factors-1 and -2*. Science, 1993. **259**(5097): p. 971.

- 483 9. Doherty, G.M., et al., *Interferon regulatory factor expression in human breast cancer*.  
484 *Annals of surgery*, 2001. **233**(5): p. 623-629.
- 485 10. Härtlova, A., et al., *DNA Damage Primes the Type I Interferon System via the Cytosolic*  
486 *DNA Sensor STING to Promote Anti-Microbial Innate Immunity*. *Immunity*, 2015.  
487 **42**(2): p. 332-343.
- 488 11. Ranoa, D.R.E., et al., *Cancer therapies activate RIG-I-like receptor pathway through*  
489 *endogenous non-coding RNAs*. *Oncotarget*, 2016. **7**(18): p. 26496-26515.
- 490 12. Elion, D.L., et al., *Therapeutically Active RIG-I Agonist Induces Immunogenic Tumor*  
491 *Cell Killing in Breast Cancers*. *Cancer Research*, 2018. **78**(21): p. 6183.
- 492 13. Besch, R., et al., *Proapoptotic signaling induced by RIG-I and MDA-5 results in type I*  
493 *interferon-independent apoptosis in human melanoma cells*. *The Journal of Clinical*  
494 *Investigation*, 2009. **119**(8): p. 2399-2411.
- 495 14. Goubau, D., et al., *Transcriptional re-programming of primary macrophages reveals*  
496 *distinct apoptotic and anti-tumoral functions of IRF-3 and IRF-7*. *European Journal of*  
497 *Immunology*, 2009. **39**(2): p. 527-540.
- 498 15. Chattopadhyay, S., et al., *Viral apoptosis is induced by IRF-3-mediated activation of*  
499 *Bax*. *The EMBO Journal*, 2010. **29**(10): p. 1762-1773.
- 500 16. Chattopadhyay, S., et al., *Ubiquitination of the Transcription Factor IRF-3 Activates*  
501 *RIPA, the Apoptotic Pathway that Protects Mice from Viral Pathogenesis*. *Immunity*,  
502 2016. **44**(5): p. 1151-1161.
- 503 17. El Maadidi, S., et al., *A Novel Mitochondrial MAVS/Caspase-8 Platform Links RNA*  
504 *Virus-Induced Innate Antiviral Signaling to Bax/Bak-Independent Apoptosis*. *The*  
505 *Journal of Immunology*, 2014. **192**(3): p. 1171.
- 506 18. Wüst, S., et al., *Comparative Analysis of Six IRF Family Members in Alveolar*  
507 *Epithelial Cell-Intrinsic Antiviral Responses*. *Cells*, 2021. **10**(10): p. 2600.
- 508 19. Willemsen, J., et al., *Phosphorylation-Dependent Feedback Inhibition of RIG-I by*  
509 *DAPK1 Identified by Kinome-wide siRNA Screening*. *Molecular Cell*, 2017. **65**(3): p.  
510 403-415.e8.
- 511 20. Krischuns, T., et al., *Phosphorylation of TRIM28 Enhances the Expression of IFN- $\beta$*   
512 *and Proinflammatory Cytokines During HPAIV Infection of Human Lung Epithelial*  
513 *Cells*. *Front Immunol*, 2018. **9**: p. 2229.
- 514 21. Urban, C., et al., *Persistent Innate Immune Stimulation Results in IRF3-Mediated but*  
515 *Caspase-Independent Cytostasis*. *Viruses*, 2020. **12**(6).

- 516 22. Bender, S., et al., *Activation of Type I and III Interferon Response by Mitochondrial*  
517 *and Peroxisomal MAVS and Inhibition by Hepatitis C Virus*. PLOS Pathogens, 2015.  
518 **11**(11): p. e1005264.
- 519 23. Binder, M., et al., *Molecular mechanism of signal perception and integration by the*  
520 *innate immune sensor retinoic acid-inducible gene-I (RIG-I)*. The Journal of biological  
521 chemistry, 2011. **286**(31): p. 27278-27287.
- 522 24. Wang, S., et al., *Doxorubicin induces apoptosis in normal and tumor cells via distinctly*  
523 *different mechanisms. intermediacy of H(2)O(2)- and p53-dependent pathways*. J Biol  
524 Chem, 2004. **279**(24): p. 25535-43.
- 525 25. Tamura, T., et al., *An IRF-1-dependent pathway of DNA damage-induced apoptosis in*  
526 *mitogen-activated T lymphocytes*. Nature, 1995. **376**(6541): p. 596-599.
- 527 26. Hickson, I., et al., *Identification and Characterization of a Novel and Specific Inhibitor*  
528 *of the Ataxia-Telangiectasia Mutated Kinase ATM*. Cancer Research, 2004. **64**(24): p.  
529 9152.
- 530 27. Fokas, E., et al., *Targeting ATR in vivo using the novel inhibitor VE-822 results in*  
531 *selective sensitization of pancreatic tumors to radiation*. Cell Death & Disease, 2012.  
532 **3**(12): p. e441-e441.
- 533 28. Tong, A.-J., et al., *A Stringent Systems Approach Uncovers Gene-Specific Mechanisms*  
534 *Regulating Inflammation*. Cell, 2016. **165**(1): p. 165-179.
- 535 29. Cataldi, M., et al., *Breaking resistance of pancreatic cancer cells to an attenuated*  
536 *vesicular stomatitis virus through a novel activity of IKK inhibitor TPCA-1*. Virology,  
537 2015. **485**: p. 340-354.
- 538 30. Podolin, P.L., et al., *Attenuation of Murine Collagen-Induced Arthritis by a Novel,*  
539 *Potent, Selective Small Molecule Inhibitor of IκB Kinase 2, TPCA-1 (2-*  
540 *[(Aminocarbonyl)amino]-5-(4-fluorophenyl)-3-thiophenecarboxamide), Occurs via*  
541 *Reduction of Proinflammatory Cytokines and Antigen-Induced T Cell Proliferation*.  
542 Journal of Pharmacology and Experimental Therapeutics, 2005. **312**(1): p. 373.
- 543 31. Bartek, J. and J. Lukas, *Chk1 and Chk2 kinases in checkpoint control and cancer*.  
544 Cancer Cell, 2003. **3**(5): p. 421-429.
- 545 32. Schmitt, Adam M., et al., *p50 (NF-κB1) Is an Effector Protein in the Cytotoxic*  
546 *Response to DNA Methylation Damage*. Molecular Cell, 2011. **44**(5): p. 785-796.
- 547 33. King, C., et al., *Characterization and preclinical development of LY2603618: a*  
548 *selective and potent Chk1 inhibitor*. Investigational New Drugs, 2014. **32**(2): p. 213-  
549 226.

- 550 34. Norbury, C.J. and B. Zivnotovsky, *DNA damage-induced apoptosis*. *Oncogene*, 2004.  
551 **23**(16): p. 2797-2808.
- 552 35. Sistigu, A., et al., *Cancer cell—autonomous contribution of type I interferon signaling*  
553 *to the efficacy of chemotherapy*. *Nature Medicine*, 2014. **20**: p. 1301.
- 554 36. Balkwill, F., D. Watling, and J. Taylor-Papadimitriou, *Inhibition by lymphoblastoid*  
555 *interferon of growth of cells derived from the human breast*. *International Journal of*  
556 *Cancer*, 1978. **22**(3): p. 258-265.
- 557 37. Widau, R.C., et al., *RIG-I-like receptor LGP2 protects tumor cells from ionizing*  
558 *radiation*. *Proceedings of the National Academy of Sciences*, 2014. **111**(4): p. E484.
- 559 38. Chiappinelli, Katherine B., et al., *Inhibiting DNA Methylation Causes an Interferon*  
560 *Response in Cancer via dsRNA Including Endogenous Retroviruses*. *Cell*, 2015. **162**(5):  
561 p. 974-986.
- 562 39. Guo, Q., et al., *STING promotes senescence, apoptosis, and extracellular matrix*  
563 *degradation in osteoarthritis via the NF- $\kappa$ B signaling pathway*. *Cell Death & Disease*,  
564 2021. **12**(1): p. 13.
- 565 40. Harberts, E., et al., *MyD88 mediates the decision to die by apoptosis or necroptosis*  
566 *after UV irradiation*. *Innate Immunity*, 2013. **20**(5): p. 529-539.
- 567 41. Huang, T.T., et al., *Sequential Modification of NEMO/IKK $\gamma$  by SUMO-1 and Ubiquitin*  
568 *Mediates NF- $\kappa$ B Activation by Genotoxic Stress*. *Cell*, 2003. **115**(5): p. 565-576.
- 569 42. Wang, P., et al., *PUMA is directly activated by NF- $\kappa$ B and contributes to TNF- $\alpha$ -*  
570 *induced apoptosis*. *Cell Death & Differentiation*, 2009. **16**(9): p. 1192-1202.
- 571 43. Gatz, S.A. and L. Wiesmüller, *p53 in recombination and repair*. *Cell Death &*  
572 *Differentiation*, 2006. **13**(6): p. 1003-1016.
- 573 44. Boege, Y., et al., *A Dual Role of Caspase-8 in Triggering and Sensing Proliferation-*  
574 *Associated DNA Damage, a Key Determinant of Liver Cancer Development*. *Cancer*  
575 *Cell*, 2017. **32**: p. 342 - 359.e10.
- 576 45. Feng, H., et al., *Interferon regulatory factor 1 (IRF1) and anti-pathogen innate immune*  
577 *responses*. *PLOS Pathogens*, 2021. **17**(1): p. e1009220.
- 578 46. Kim, W., et al., *PIMI-Activated PRAS40 Regulates Radioresistance in Non-small Cell*  
579 *Lung Cancer Cells through Interplay with FOXO3a, 14-3-3 and Protein Phosphatases*.  
580 *Radiation Research*, 2011. **176**(5): p. 539-552.
- 581 47. Yang, H.J., et al., *Investigation of Radiation-induced Transcriptome Profile of*  
582 *Radioresistant Non-small Cell Lung Cancer A549 Cells Using RNA-seq*. *PLOS ONE*,  
583 2013. **8**(3): p. e59319.



- 584 48. Pawlik, A., et al., *Transcriptome Characterization Uncovers the Molecular Response*  
585 *of Hematopoietic Cells to Ionizing Radiation*. Radiation Research, 2010. **175**(1): p. 66-  
586 82.
- 587 49. Zhang, Q., et al., *Integrating radiosensitive genes improves prediction of*  
588 *radiosensitivity or radioresistance in patients with oesophageal cancer*. Oncology  
589 letters, 2019. **17**(6): p. 5377-5388.
- 590 50. Jones, K.B., et al., *miRNA signatures associate with pathogenesis and progression of*  
591 *osteosarcoma*. Cancer research, 2012. **72**(7): p. 1865-1877.
- 592 51. Negishi, H., et al., *Evidence for licensing of IFN- $\gamma$ -induced IFN regulatory factor 1*  
593 *transcription factor by MyD88 in Toll-like receptor-dependent gene induction*  
594 *program*. Proceedings of the National Academy of Sciences, 2006. **103**(41): p. 15136.
- 595 52. Wang, J., et al., *IRF1 Promotes the Innate Immune Response to Viral Infection by*  
596 *Enhancing the Activation of IRF3*. Journal of Virology, 2020. **94**(22): p. e01231-20.
- 597 53. Bouker, K.B., et al., *Interferon regulatory factor-1 (IRF-1) exhibits tumor suppressor*  
598 *activities in breast cancer associated with caspase activation and induction of*  
599 *apoptosis*. Carcinogenesis, 2005. **26**(9): p. 1527-1535.
- 600 54. Kim, P.K.M., et al., *IRF-1 expression induces apoptosis and inhibits tumor growth in*  
601 *mouse mammary cancer cells in vitro and in vivo*. Oncogene, 2004. **23**(5): p. 1125-  
602 1135.
- 603 55. Tan, L., et al., *Interferon regulatory factor-1 suppresses DNA damage response and*  
604 *reverses chemotherapy resistance by downregulating the expression of RAD51 in*  
605 *gastric cancer*. Am J Cancer Res, 2020. **10**(4): p. 1255-1270.
- 606 56. Thyrell, L., et al., *Mechanisms of Interferon-alpha induced apoptosis in malignant*  
607 *cells*. Oncogene, 2002. **21**(8): p. 1251-1262.
- 608 57. Choi, E.A., et al., *Stat1-dependent Induction of Tumor Necrosis Factor-related*  
609 *Apoptosis-inducing Ligand and the Cell-Surface Death Signaling Pathway by*  
610 *Interferon  $\beta$  in Human Cancer Cells*. Cancer Research, 2003. **63**(17): p. 5299.
- 611 58. Kok, F., et al., *Disentangling molecular mechanisms regulating sensitization of*  
612 *interferon alpha signal transduction*. Molecular systems biology, 2020. **16**(7): p.  
613 e8955-e8955.
- 614 59. Nan, J., et al., *TPCA-1 Is a Direct Dual Inhibitor of STAT3 and NF- $\kappa$ B and Regresses*  
615 *Mutant EGFR-Associated Human Non-Small Cell Lung Cancers*. Molecular Cancer  
616 Therapeutics, 2014. **13**(3): p. 617.



617 **Acknowledgements**

618 We want to thank Joschka Willemsen and Leanne Strauß for having started our lab's research line on  
619 RLR-related cell death and providing valuable preliminary data, Hendrik Welsch for help with the  
620 IncuCyte instrument and fruitful discussions, Volker Lohmann and Charlie Rice for provision of cell  
621 lines, and Ralf Bartenschlager for providing an excellent research environment and supervising the  
622 doctoral thesis of D.Z.. We are grateful to Eva Schnober, Hartmut Hengel and the rest of the team for  
623 managing the fantastic Integrated Research Training Group "Immunovirology" as part of TRR179,  
624 supporting D.Z. with a doctoral fellowship.

625 **Conflicts of interest**

626 The authors declare no conflict of interest.

627 **Author contributions**

628 This study was conceived and designed by M.B. and D.Z., critical intellectual input was provided by  
629 V.G.M., experiments were performed by D.Z. with assistance and contributions by S.W., S.S.B. and  
630 M.G.V., data was evaluated by D.Z. and M.B., the manuscript was written by D.Z. and M.B. and edited  
631 and approved of by all authors.

632 **Ethics Approval**

633 This research did not involve human or animal material; ethical approval was not required.

634 **Funding**

635 This research was funded by the German Research Foundation (Deutsche Forschungsgemeinschaft,  
636 DFG), project BI1693/1-2 and project 272983813 CRC-TR 179 (TP11).

637 **Data Availability**

638 The raw data acquired for this study are available from the corresponding author on reasonable request.